Journal of Agronomy and Crop Science

WILEY

Journal of Agronomy and Crop Science

ORIGINAL ARTICLE OPEN ACCESS

Unravelling Compositional Changes in Field Pea Leaf Cuticles Under Heat Stress Using Synchrotron-Based Fourier Transform Mid-Infrared Spectroscopy

Yunfei Jiang[1] | Rachid Lahlali[2] | Rosalind Bueckert[1] | Saroj Kumar[2] | Chithra Karunakaran[2]

[1]Department of Plant Sciences, University of Saskatchewan, Saskatoon, Saskatchewan, Canada | [2]Canadian Light Source Inc, Saskatoon, Saskatchewan, Canada

Correspondence: Yunfei Jiang (yunfei.jiang@dal.ca)

Received: 28 March 2025 | **Revised:** 28 March 2025 | **Accepted:** 3 April 2025

Funding: This work was supported by Saskatchewan Agriculture Development Fund; Saskatchewan Pulse Growers Association; Western Grains Research Fund; Natural Sciences and Engineering Research Council of Canada; Canada Foundation for Innovation; National Research Council Canada; Canadian Institutes of Health Research; Western Economic Diversification Canada; Canadian Light Source Inc; University of Saskatchewan.

Keywords: heat stress | infrared spectroscopy | leaf cuticle | oxidative stress | *Pisum sativum*

ABSTRACT

Plant leaf cuticle, a heterogeneous and lipophilic membrane, is an interface between the plant and its aerial environment and protects plants against abiotic and biotic stresses. This study used synchrotron-based Fourier transform mid infrared (sFTIR) spectroscopy to evaluate the effect of heat stress on the compositional changes of leaf cuticles in field pea (*Pisum sativum*). The results showed that oxidative stress was associated with heat stress. A new peak at 1721 cm^{-1} was observed in the heat-stressed leaf cuticles, and it was not found in the control leaf samples; this peak arises from the carbonyl stretching (C=O) from the aldehyde of 4-Hydroxynonenal (4-HNE) which is an adduct of the lipid peroxidation chain reaction. Heat stress reduced the amounts of phenolic compounds in leaf cuticles, indicated by the reduction of the integrated band area in the region of 1650–1500 cm^{-1}. Substantial spectral variations between the control and heat-stressed leaf cuticles were revealed using Principal Component Analysis (PCA). The spectral information showed the compositional changes in waxes, cutin, cutan, phenolic compounds and polysaccharides may be due to heat stress. This study provides important information for rapid understanding of the compositional changes of leaf cuticles under environmental stresses and may significantly contribute to routine screening for resistant pea genotypes to heat stress.

1 | Introduction

Field pea (*Pisum sativum*) is an economically important crop in western Canada, where heat stress is one of the major environmental stresses affecting crop production under the semi-arid agricultural conditions. Canada is one of the leading producers of dry peas with a total production of 3.42 million tonnes in 2022, along with other major dry pea producing countries of Russia, China and India (FAOSTAT 2024). Pea cultivars are generally heat-sensitive; over 20 days of above 28°C reduces the number of days spent in reproductive growth (from initiation of flowering to seed maturity) and yield under dryland conditions of Saskatchewan (Bueckert et al. 2015). Similarly, an increase in the maximum temperatures over 25°C during the flowering stage caused yield loss in pea under field conditions (Sadras et al. 2012). Controlled high temperatures decrease in vitro pollen germination, pollen viability, pollen tube growth, the proportion of ovules that received a pollen

Yunfei Jiang and Rachid Lahlali are equal contributions.

This is an open access article under the terms of the Creative Commons Attribution License, which permits use, distribution and reproduction in any medium, provided the original work is properly cited.

© 2025 The Author(s). *Journal of Agronomy and Crop Science* published by Wiley-VCH GmbH.

Summary

- Heat stress-induced pea leaf cuticle composition changes were detected using synchrotron-based FTIR.
- Heat stress caused compositional changes in waxes, cutin, cutan, phenolic compounds and polysaccharides.
- Heat stress resulted in oxidative stress in pea leaf cuticles.

tube, seed-ovule ratio, pod length and the number of seeds per pod in field pea (Jiang, Bueckert, et al. 2017; Jiang, Davis, et al. 2019, 2020; Jiang, Diapari, et al. 2017; Jiang et al. 2015; Jiang, Lahlali, et al. 2019; Jiang, Lindsay, et al. 2020). Previous research conducted using Mid-IR spectroscopy showed that modifications of anther, pollen surface lipid and pollen surface protein compositions in field pea were involved with heat stress conditions (Jiang et al. 2015; Jiang, Lahlali, et al. 2019; Lahlali et al. 2014).

Cuticles protect plants from uncontrolled loss of water as well as against abiotic and biotic stresses. Plant cuticles consist of three distinctive layers including epicuticular wax (EW), cuticle proper (CP) and cuticular layer (CL). The main chemical compositions of plant cuticles consist of cutin (C_{16} and C_{18} hydroxyalkanoic acids), cutan, epicuticular waxes, intracuticular waxes, phenolics (such as cinnamic acids and flavonoids) and polysaccharides (Domínguez et al. 2011; Shepherd and Wynne Griffiths 2006; Villena et al. 2000). Epicuticular waxes at a leaf outermost layer (a hydrophobic layer) provide a protective barrier when plants are exposed to various abiotic and biotic stresses (Shepherd and Wynne Griffiths 2006). The epicuticular wax layer (soluble cuticular lipids) consists primarily of long-chain hydrocarbon compounds including alkenes, primary alcohols, aldehydes, secondary alcohols, ketones, esters and other derived compounds (Shepherd and Wynne Griffiths 2006). Hydrocarbons, alkyl esters, primary alcohols, fatty acids and possibly ketones were detected on the leaf surface waxes in *Pisum sativum* (Gonzalez et al. 1996; Hall et al. 1965). Polysaccharides detected in cuticles included cellulose, hemicelluloses and pectin, which are similar to those polysaccharides found in the cell wall (Guzmán, Fernández, García, et al. 2014).

Fourier transform mid infrared (FTIR) spectroscopy is a rapid and non-invasive vibrational spectroscopic technique that provides a snapshot of tissue metabolic composition, which is yet to be fully utilised in plant science research (Götz et al. 2020; Innes et al. 2019; Liu et al. 2019, 2020; Martin et al. 2005; McCann et al. 1997; Tanino et al. 2017). The FTIR generates a spectrum of vibrating molecules excited by infrared light, providing a biochemical fingerprint of the sample under investigation. A range of functional groups, including carbonyl esters, phenolic esters, protein amides and carboxylic acids, absorb infrared radiation at characteristic frequencies and thus are clearly resolved in the spectrum (Chen et al. 1998). The configuration of molecular functions in a sample can be investigated using the infrared absorption peak width, position and intensity (Yee et al. 2004). Therefore, changes due to specific experimental treatments can be detected through changes in some of the absorption peaks (Freitas et al. 2008). The application of FTIR spectroscopy to analyse plant cuticles has been conducted in several plant species, such as *Eucalyptus botryoides* (Heraud et al. 2007); *Lycopersicon esculentum* and *Beta vulgaris* (Ribeiro da Luz 2006); *Eucalyptus camaldulensis* and *Eucalyptus globulus* (Guzmán, Fernández, Graça, et al. 2014); *Spinacia oleracea* (Hardin 2012); *Allium fistulosum* (Tanino et al. 2013); *Clivia miniata* (Villena et al. 2000); *Humulus lupulus* (Dubis et al. 2001); *Solanum lycopersium* (España et al. 2014; Heredia-Guerrero et al. 2012); *Allium cepa* (Götz et al. 2020); *Pisum sativum* (Innes et al. 2019; Liu et al. 2019); *Lycopersicon esculentum*, *Capsicum anuum*, *Malus pumila* and *Olea europaea* (Johnson et al. 2007).

Globar and a synchrotron beam are two different light sources for FTIR spectroscopy. The synchrotron source is 100–1000 times brighter than a conventional (globar) source (Dokken et al. 2005). There is a trade-off between spatial resolution and spectral acquisition. Compared to conventional globar IR spectroscopy, synchrotron-based IR spectroscopy enables faster spectral acquisition at the same level of signal-to-noise. In other words, synchrotron-based IR spectroscopy allows for measurement with high spatial resolution spectroscopy with the same amount of time (Carr 2001; Isensee et al. 2018; Pellerin et al. 2004; Teng et al. 2024; Wang et al. 2022). A chemical map linking chemical information from infrared absorbance with spatially localised information can be established using FTIR. The Attenuated Total Reflection (ATR) FTIR spectroscopy without the synchrotron light was used to quantify the changes of pea leaf adaxial cuticles (Liu et al. 2019) and wheat (*Triticum aestivum*) (Willick et al. 2018). However, the higher resolution of FTIR spectroscopy with the synchrotron light source in pea has not been investigated.

Conventional wet chemistry analysis of leaf cuticles requires isolation and purification of cuticular components. Organic solvent extraction has been commonly used to isolate cuticular components such as waxes and phenolic compounds. Those organic solvents are usually environmental pollutants and cause potential health hazards. The organic solvents may also interfere with targeted compounds, leading to the degradation of cuticular components (Khoddami et al. 2013). These procedures are often invasive and destructive to plant tissue, and they require substantial sample preparation and are time-consuming. Therefore, a novel and rapid method with minimum sample preparation is required.

This present work filled the gap by introducing a novel technique to obtain leaf cuticle characterisation without cuticle isolation and purification using organic solvents. The aim of this work was to elucidate compositional changes in leaf surface tissue related to heat stress using this rapid and non-destructive technique—synchrotron-based FITR (sFTIR) spectroscopy.

2 | Materials and Methods

2.1 | Experiment 1—Leaf Cuticle Composition Using sFTIR

Field pea plants (cv. CDC Golden) were grown in the field at Saskatoon (52.1333° N, 106.6833° W), Saskatchewan during the 2015 growing season. Main branches from six plants were collected and incubated at 24°C and 42°C for 5 h at the early reproductive stage when flowers at the first or second fruiting

nodes were open. The epidermal layer was peeled from newly fully expanded leaves (usually the third node counted from the top of main branch) from different temperature treatments with three replications (one leaf from one branch per plant at one temperature regime, either 24°C or 42°C, was considered as one replication). A drop of distilled water was added to the CaF_2 slide (2 mm thick, 25 mm diameter), and the epidermal layer was placed on the surface of the CaF_2 slide due to the hydrophilism of newly peeled leaf surfaces. Leaf samples were air-dried to reduce moisture content. The sFTIR spectroscopy data collection was conducted at the mid-infrared beamline (01B1-1) at the Canadian Light Source using a Hyperion 3000 microscope (Bruker Optics Inc., Milton, ON, Canada) equipped with a cryo-cooled single element MCT (HgCdTe) detector. Spectra were recorded in transmission mode using a 36× IR objective at a spectral resolution of 4 cm^{-1} with an aperture size of 10 × 10 μm. A total of 256 scans were averaged for each spectrum. The background spectra were recorded from a sample-free area on the window.

Average spectra and second derivatives spectra of three leaf replications for each treatment (total of 6 leaf samples, approximately 15 spectra for each sample) were calculated and a baseline correction was applied using the OPUS software (version 7.0, Bruker Optics Inc. Billerica, MA, USA). The 1800–1500 cm^{-1} region, where important chemical compositions such as phenolic compounds responding to heat stress are located, was highlighted and analysed using curve fitting with a program called Kinetics, written by Goormaghtigh et al. (2006) using Matlab (version R2008, Mathworks Inc.). Curve fitting is a statistical analysis to resolve the component bands and to quantify their contributions. The details of the curve fitting analysis are described in Lahlali et al. (2014). Principal Component Analysis (PCA) was performed using the Unscrambler software (version 10.1, Camo Software AS., Norway). PCA is a commonly used method in infrared spectroscopy to observe the variability within and between samples. PCA can be used to reduce the number of variables and to provide an easy graphical representation on the spread of data (Szymanska-Chargot and Zdunek 2013). Before PCA analysis, individual spectral data were smoothed over 9 points by Savitzki-Golay (SG) algorithm method. PCA was performed on the data by considering each wavelength of FTIR treated as an equally weighted variable. The first PC axis shows the direction of greatest variability; the second greatest variance can be observed from the second PC axis and so on. Score plots were used to visualise clusters of the data, and loading plots were used to determine the spectral region, which contributed to the greatest variance in the dataset.

2.2 | Experiment 2—Leaf Surface Morphology

Newly fully expanded leaves (usually the third node counted from the top of main branch) from the control growth chamber (24/18°C day/night temperatures for 4 days, 16/8 h photoperiod) and the high temperature chamber (35/18°C day/night temperatures for 4 days, 16/8 h photoperiod) at the anthesis stage of CDC Golden (4 replications per treatment) were collected for leaf surface observation using a scanning electron microscope (SEM). Leaf samples were freeze-dried for 24 h, and they were coated with a thin layer of gold–palladium using a Sputter coater (Edwards S150B Sputter Coater, Wilmington, MA) before examination using a SEM (Phenom, G_2Pure), and imaged using a charge-coupled device (CCD) navigation camera.

3 | Results and Discussion

3.1 | High Wavenumber Region of sFTIR Spectra

The microscopic images of the control and heat-stressed leaf cuticles analysed using sFTIR were shown in Figure 1a,c. The average infrared spectrum of the control and the heat-stressed leaf cuticles with the presence of many strong absorption bands from different chemical components was shown in Figure 1b,d. The high wavenumber region (3000–2750 cm^{-1}, shorter wavelengths) consists of bands from asymmetric CH_2 (2918 cm^{-1}), symmetric CH_2 (2850 cm^{-1}) (Figure 1 and Table 1) and is consistent with the results of FTIR spectra of leaf cuticles of *Eucalyptus camaldulensis*, *Eucalyptus globulus*, *Buxus sempervirens*, *Ficus elastica*, *Ilex aquifolium*, *Prunus lauroerasus*, *Vanilla* sp. and *Solanum lycopersicum*. These plant species have characteristic intense and thin bands of long-chain linear aliphatic compounds (Guzmán, Fernández, Graça, et al. 2014; Heredia-Guerrero et al. 2014). The second derivatives of the average absorption spectra for better separation of overlapping peaks were shown in Figure 2. Two strong negative peaks were obvious at 2919 cm^{-1} (asymmetrical CH_2) and 2850 cm^{-1} (symmetrical CH_2) in the higher wavenumber region (Figure 2a).

PCA was conducted to extract relevant information between the control leaf cuticles and the heat-stressed samples (Figure 3). Two groups of the control and heat-stressed leaf cuticles can be separated by the first principal component (PC) score that accounted for 81% of the total spectral variation (Figure 3a). Similarly, the grouping information in Figure 3b was consistent with the results in Figure 3a that PC1 separated the control and heat-stressed samples. PC loadings (Figure 3c–e) represent an independent source of spectral variation, which produce a mathematically derived spectrum. In the high wavenumber region (3100–2750 cm^{-1} in Figure 3c), bands causing the major variation in the PC1 axis included asymmetric CH_2 (2918 cm^{-1}) and symmetric CH_2 (2850 cm^{-1}) vibrations. The data showed that bands at 2918 and 2850 cm^{-1} were attributable to waxes. Other chemical components causing small variation in the PC1 of the PCA separation included those bands at 2958 (stretching vibrations of CH_3, a small shoulder to stretching vibrations of CH_2 at 2918 cm^{-1}), 2930 (stretching vibrations of methylene groups), 2906, 2861 and 2838 cm^{-1} (Figure 3c). Bands at 2925 (stretching vibrations of CH_2), 2912, 2856 (stretching vibrations of CH_2) and 2842 cm^{-1} were major chemical groups leading to the variation in the PC2 in the high wavenumber region (Figure 3d).

3.2 | Low Wavenumber Region of sFTIR Spectra

In the low wavenumber region (1800–800 cm^{-1}) of the average infrared spectrum (Figure 1b,d), C=O stretching vibration of an alkyl ester (1737–1732 cm^{-1}) was accompanied by two bands near 1165 and 1118 cm^{-1} due to asymmetrical and symmetrical

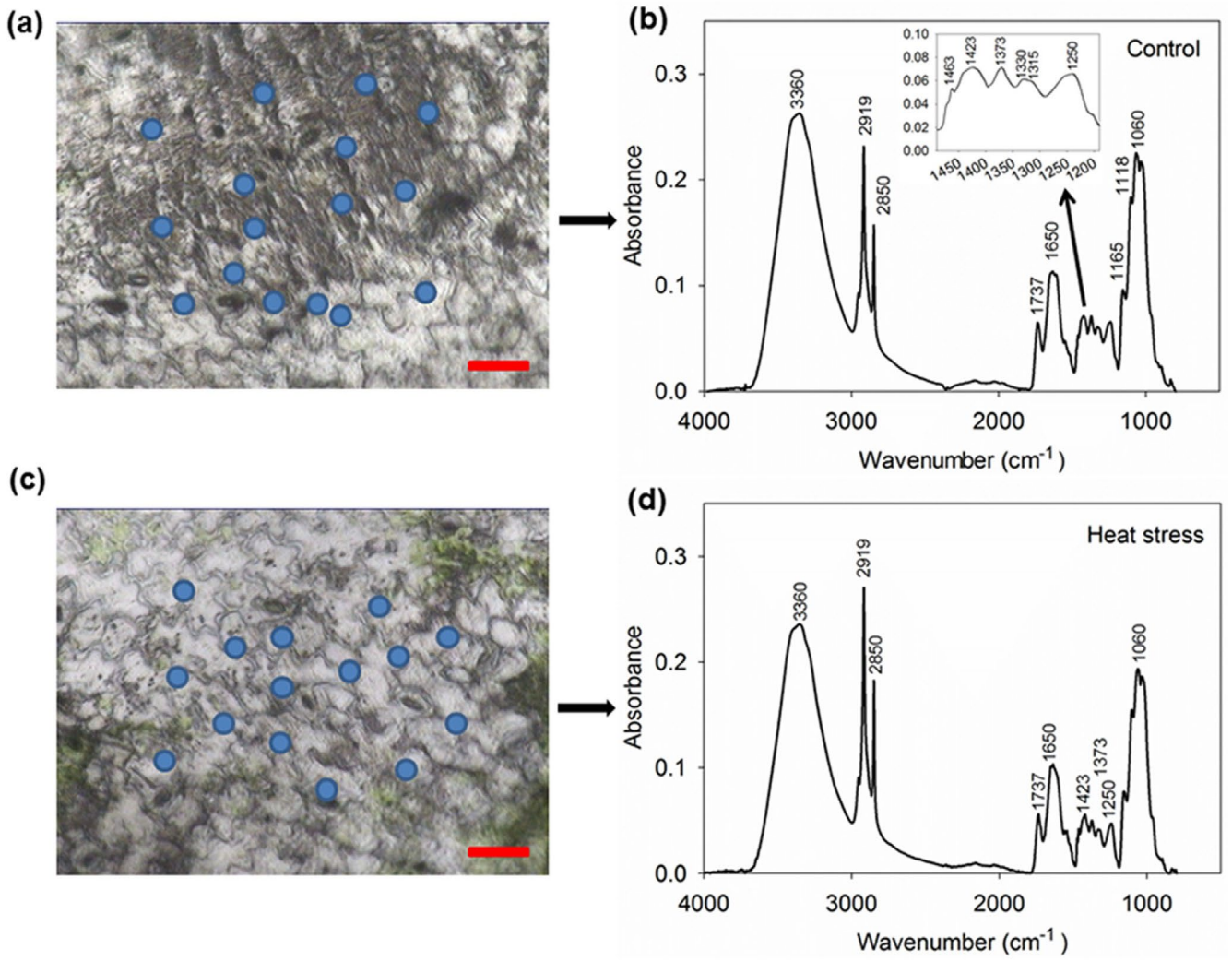


FIGURE 1 | Microscopic images and average sFTIR spectra of control and heat-stressed leaf cuticles of *Pisum sativum* cv. CDC Golden. (a and b): Microscopic image and average spectra of control leaf cuticles (24°C for 5 h); (c and d): Microscopic image and average spectra of heat-stressed leaf cuticles (42°C for 5 h). (a and c): Data are means of approximately 45 individual spectra from 3 replications for each treatment. (b and d): Each blue dot (256 scans) represents a location in the leaf sample where a spectrum from the whole region (4000–800 cm^{-1}) was generated. Location and size of the blue dots (a, c) were for illustration purposes, rather than the actual sampling location size. Scale bar = 50 μm.

C-O-C stretching ester vibrations. The identification of these bands was similar to the results described by Heredia-Guerrero et al. (2014). The C=C stretching (1658–1500 cm^{-1}) band can be attributed to aromatic structures of phenolic compounds (Heredia-Guerrero et al. 2014); the band at 1463 cm^{-1} indicates CH_2 scissoring and rocking vibrations (Figure 1 and Table 1). In the lower wavenumber region (1800–800 cm^{-1}) of the second derivatives (Figure 2b,c), there were many peaks corresponding to the absorption spectra: 1737, 1720, 1652, 1650, 1544, 1514, 1468, 1374, 1235, 1163, 1108 and 828 cm^{-1} (Figure 2b); and their corresponding band assignments are listed in Table 1. In the low wavenumber region of PCA results (Figure 3d,e), many chemical components are involved causing variation in the PCA separation. Bands causing major variation in the PC1 in the low wavenumber region include 1608 (phenolic compounds), 1542 (related to protein—amide II band), 1487, 1472, 1449, 1127, 1110, 1091, 1076 and 992 cm^{-1} (Figure 3d and Table 1), and peaks leading to major variation in the PC2 in the low wavenumber region include 1654 (phenolic compounds), 1485, 1184, 1165, 1142, 1110 and 1095 cm^{-1} (Figure 3e).

The integrated area near 1737 cm^{-1} (ascribing to the stretching of C=O in ester groups) of leaf cuticles under control conditions was greater than that with heat stress treatment (Figure 4 and Table 2). The ester carbonyl (C=O) stretching band at around 1740 cm^{-1} has been used to determine membrane phase transition temperature values (Tm, the midpoint between gel and liquid crystal frequencies) of lipids, which are membrane-specific and also focus on the polar interfacial region (Mantsch et al. 1988; Sowa et al. 1991).

3.3 | Oxidative Stress Involved With Heat Stress

Leaf cuticles under high temperature treatments produced a new peak at 1721 cm^{-1}, and this peak was not observed in the control leaf cuticle samples (Figure 2d and Table 2). The carbonyl (C=O) vibration of COOH and esters usually occurs between 1760 and 1728 cm^{-1} (Sowa et al. 1991) and at 1721 cm^{-1} (Chai et al. 2007; Wang et al. 2014). Lipid-carbonyl groups at the band at 1720 cm^{-1} arise from products of lipid oxidation

TABLE 1 | Spectral assignment of peaks with strong absorbance in the average spectra of pea leaf surface tissue.

Leaf tissue in *Pisum sativum*		References	
Peak region or center (cm^{-1})	**Assignment**	**Peak region or center (cm^{-1})**	**Compound**
~3360	ν(O-H···O)	3304–3390	Cutin, polysaccharides[a], tissue hydration[b]
2958	$\nu_a(CH_3)$[1]		
2912–2930	$\nu_a(CH_2)$	2916–2927	Cutin[a,b], waxes[a-c], cutan[a,b]
2838–2850	$\nu_{as}(CH_2)$	2846–2853	Cutin[a], waxes[a,c]
1737–1732	ν(C=O) ester	1728–1732	Cutin[a,f]; Waxes[c]
1721	ν(C=O)		
1658–1515	ν(C-C) aromatic	1650–1500	Phenolic compounds[a,f,e]
1463–1468	$\delta_{scis}(CH_2)$ and $\delta_{rock}(CH_2)$	1462–1463	Soluble lipids[b]; nonacosane[d]
	$\delta(CH_2)$ (corresponding to ~2918 and 2850)	1468	Cutin, waxes, cutan[a]
1427–1419	δ(C-H)	1430	Suberin, cutin[a]
1375–1369	$\delta(CH_2)$ wagging and twisting	1367	Cutin, waxes[a]
1332–1327	$\delta(CH_2)$ bending stretching	1323	Cutin, waxes[a]
1243–1235	ν(C-O)	1247	Polysaccharides[f]
	δ(OH)	1243–1278	Cutin, polysaccharides[a]
1160–1165	ν_a(C–O–C)	1161–1167	Cutin[a], Cutin[f]
1118	ν(C–O–C)		
1107–1110	ν_a(C–O–C) and ν_{as}(C–O–C)	1104–1105	Esteried soluble lipids, cutin[a]
1066–1067	ν(C-O), ν(C-C)		Polysaccharides[f]
1034–1032	ν(C–O–C)	1030–1032	Glycosidic bonds type of polysaccharides[a]; Cellulose[d]
		1030	Polysaccharides[f]
992	H-O deformations	997	Polysaccharides[f]
828	γ(C-H) aromatic	833–834	Phenolic compounds[a]

Abbreviations: as, asymmetric vibrations; s, symmetric vibrations; γ, out-of-plane bending; δ, bending vibrations; ν, stretching vibrations.
[a]Leaf cuticles (Heredia-Guerrero et al. 2014).
[b]Leaf cuticle in *Eucalyptus camaldulensis* and *Eucalyptus globulus* (Guzmán, Fernández, García, et al. 2014; Guzmán, Fernández, Graça, et al. 2014).
[c]Leaf cuticle in *Spinacia oleracea* (Hardin 2012).
[d]Cellulose extraction from *Olea europea* leaf (Ribeiro da Luz 2006).
[e]Cuticles in *Clivia miniata* (Villena et al. 2000).
[f]Johnson et al. (2007).

(Borchman and Sinha 2002; Van de Voort et al. 1994). This peak (1721 cm^{-1}) in the heat-stressed leaf cuticles may arise from carbonyl stretching from the aldehyde of 4-Hydroxynonenal (4-HNE). This peak may also be associated with the peak at 1419 cm^{-1} (C-H stretching from CH_3 of 4-HNE) in the heat-stressed leaf cuticles arising from. The amount of 4-HNE increased under oxidative stress because of an increase in the lipid peroxidation chain reaction. Plants under heat stress generate excess reactive oxygen species (ROS) such as singlet oxygen ($^1O_2$), superoxide radical ($^{\cdot}O_2^-$), hydrogen peroxide (H_2O_2) and hydroxyl radical ($OH^{\cdot}$), leading to oxidative stress (Asada 2006). Singlet oxygen can cause oxidation of proteins, polyunsaturated fatty acids and DNA (Møller et al. 2007). Hydroxyl radicals can possibly react with many biomolecules such as pigments, proteins, lipids and DNA, as well as almost all cellular organelles (Karuppanapandian et al. 2011).

3.4 | Phenolic Compounds Under Heat Stress

The bands in the 1650–1500 cm^{-1} region are attributable to aromatic and C=C functional groups from phenolic compounds in plant cuticles (Heredia-Guerrero et al. 2014; Johnson et al. 2007). Integrated areas of bands at 1655, 1602, 1545 and 1515 cm^{-1} reduced under heat stress compared to the control conditions (Figure 5 and Table 2), which indicated

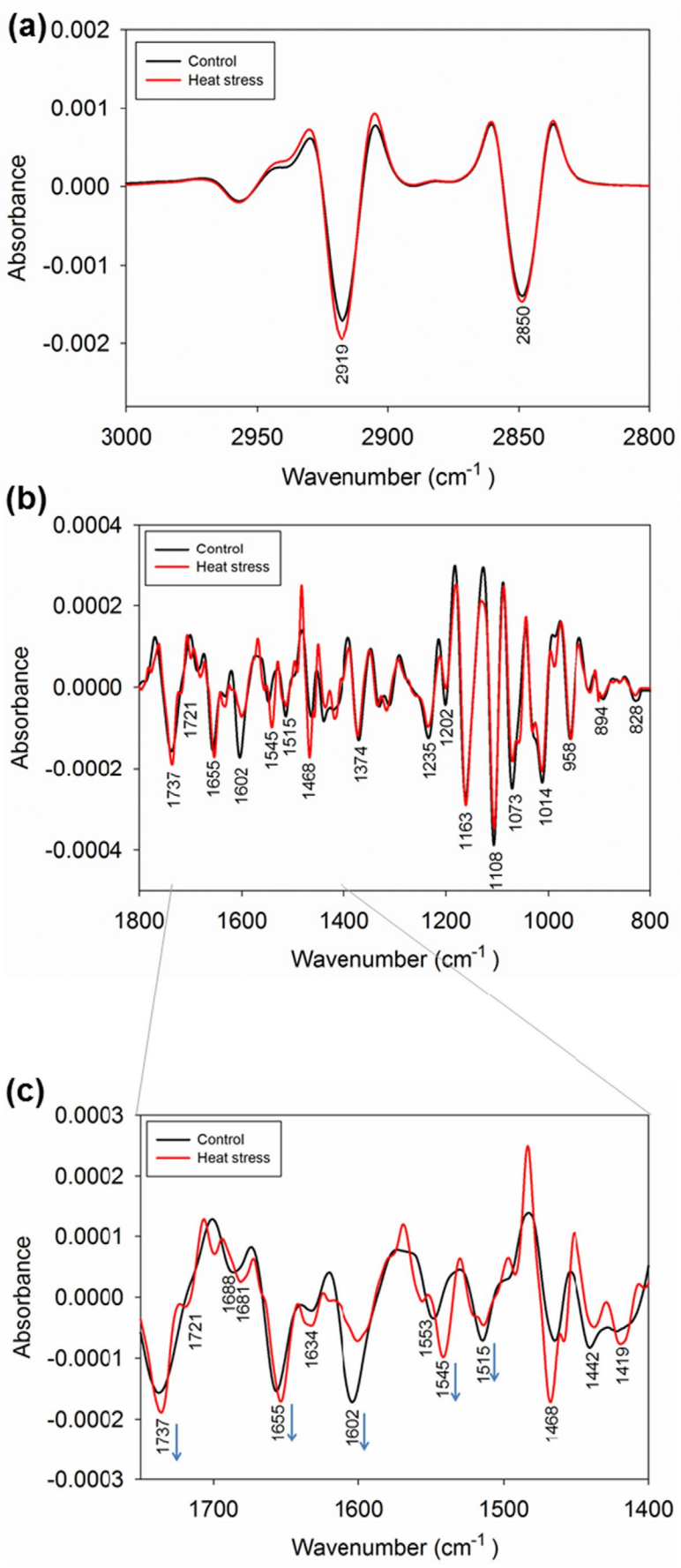


FIGURE 2 | Legend on next page.

FIGURE 2 | The average second derivative spectra of control and heat-stressed leaf cuticles of *Pisum sativum* cv. CDC Golden. The control temperature treatment is 24°C for 5 h; the heat-stressed treatment is 42°C for 5 h. Data are means of approximately 45 individual spectra from 3 replications for each treatment. (a) High wavenumber region (3000–2800 cm^{-1}); (b) Low wavenumber region (1800–800 cm^{-1}); (c) 1750–1400 cm^{-1} region.

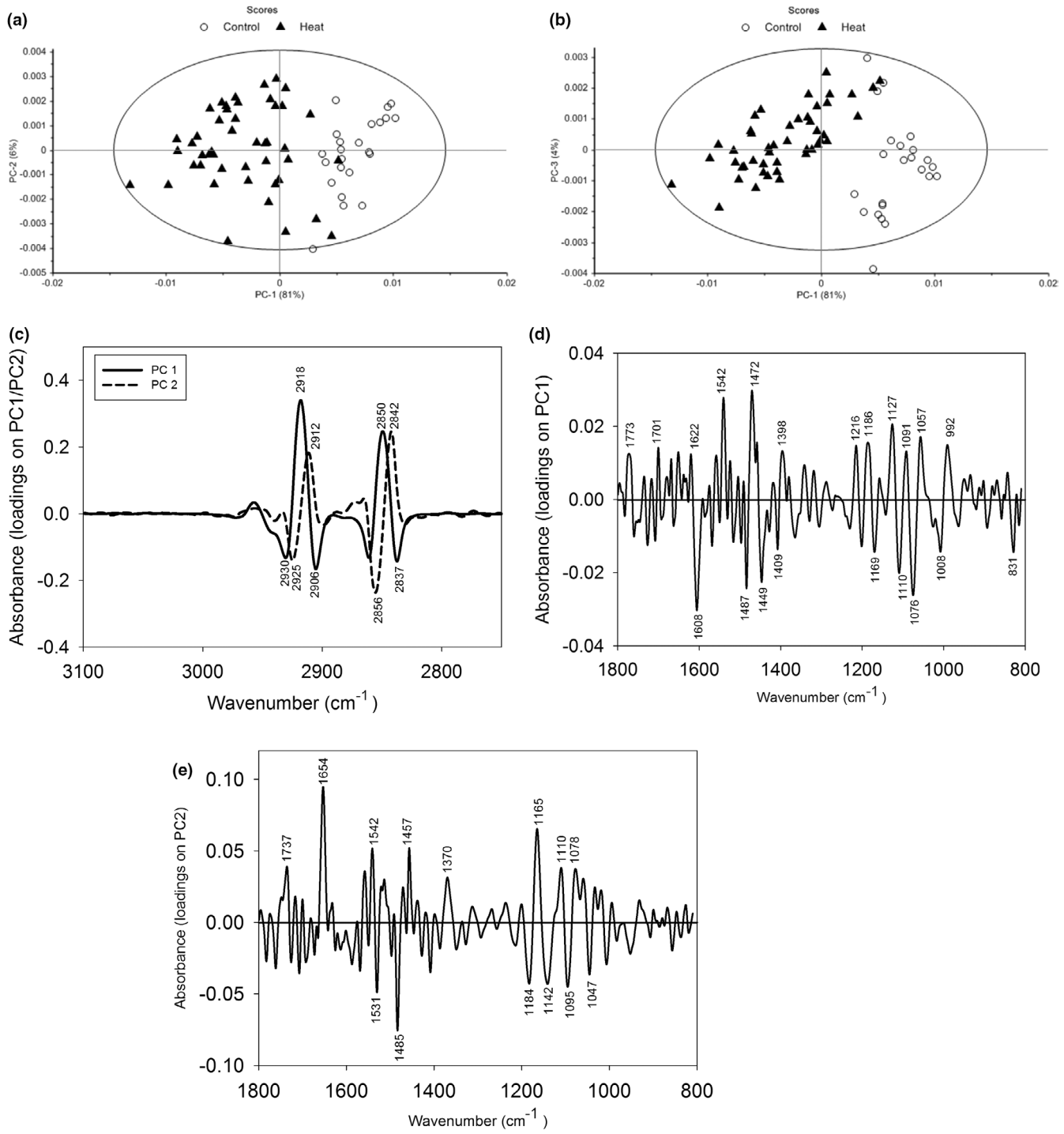


FIGURE 3 | Score plots and loading plots of the principal components (PCs). The control temperature treatment is 24°C for 5 h; the heat-stressed treatment is 42°C for 5 h. (a) Score plot of PC1 and PC2 of sFTIR spectra in control and heat-stressed leaf upper cuticles in the whole region (3800–800 cm^{-1}); (b) Score plot of PC1 and PC3 of sFTIR spectra in control and heat-stressed leaf upper cuticles (3800–800 cm^{-1}). (c) The loading plots of PC1 and PC2 in the lipid region (3100–2750 cm^{-1}); (d) The first PC loading plot in the fingerprint region (1800–800 cm^{-1}); (e) The second PC loading plot in the fingerprint region (1800–800 cm^{-1}).

the amounts of phenolic compounds in pea leaf cuticles decreased under heat stress. Similarly, a reduction of phenolic compounds under environmental stress has been documented (Król et al. 2014). A reduction of phenolic compounds in *Vitis vinifera* leaves and roots is observed under drought stress (Król et al. 2014). One potential explanation is that oxidative stress caused by heat stress led to the production of reactive oxygen species, which damaged plant metabolism, including the synthesis of phenolic compounds. Similarly, a reduction of phenolic compounds under environmental stress has been documented (Król et al. 2014). On the contrary, an increase in phenolic compounds in a cell under environmental stresses has also been reported (Wróbel et al. 2005).

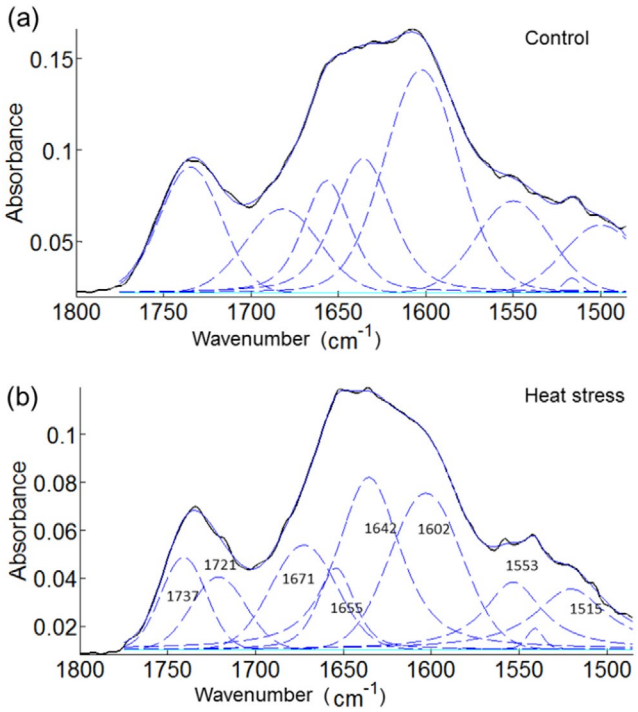


FIGURE 4 | Curve fitting of the 1800–1500 cm^{-1} region of *Pisum sativum* cv. CDC Golden control (24°C for 5 h) and heat-stressed (42°C for 5 h) leaf cuticles. Data were means of approximately 45 individual spectra from 3 replications for each treatment.

3.5 | Protein Detected in Leaf Surface Tissue

Due to cuticle's proximity to epidermal cell wall, it was likely that other compounds found at cell wall such as proteins were detected by sFTIR since transformation mode of detector was used in the present study. In protein-rich samples, the amide I band (1700–1600 cm^{-1}) primarily arises from the C=O stretching vibration, and the amide II band (1700–1500 cm^{-1}) is mainly due to the N-H bending and C-N stretching vibration (Kumar 2014; Kumar and Barth 2010; Sowa et al. 1991). In this case, chemical components at the amide I might overlap with phenolic components in leaf cuticles, but minor peaks at the amide II region are also detected (Figure 5), which suggests minor amounts of protein are observed in the pea leaf surface tissue.

3.6 | Leaf Surface Morphology (Experiment 2)

No morphological differences between the control surface (24/18°C day/night temperatures for 4 days) leaf and the heat-treated surface (35/18°C day/night temperatures for 4 days) leaf upper surface in CDC Golden were observed (Figure). Pea leaf surface consists of irregularly shaped cells with interspersed stomata (Figures 1a,c and 5). Epicuticular wax crystalloids are non-oriented at the leaf surface. The density of the wax crystalloids was very high so that the surface cell layer was not visible.

4 | Conclusions

The results in the present work have highlighted significant differences between the control and heat-stressed leaf cuticle composition. Main differences between the control and heat-stressed leaf cuticles were ascribed to cutin, cutan, waxes and phenolic compounds. In the high wavenumber region (3100–2750 cm^{-1}), the most prominent peaks that may play a role in heat stress tolerance were asymmetrical and symmetrical stretching CH_2 (2918 and 2850 cm^{-1}) vibrations. Heat stress decreased the amounts of phenolic compounds in pea leaf cuticles. Heat stress generated secondary oxidative stress—a new peak at 1721 cm^{-1} was generated in the heat-stressed leaf surface tissue, which arises from the carbonyl stretching from the aldehyde of 4-Hydroxynonenal (4-HNE) which is an adduct of the lipid peroxidation chain reaction. These results demonstrated that cutin,

TABLE 2 | Integrated area of control and heat stressed *Pisum sativum* leaf cuticles in the region of 1800–1500 cm^{-1}.

		Width		Integrated area	
Wavenumber (cm^{-1})	**Band assignment**	**Control**	**Heat stress**	**Control**	**Heat stress**
1515	ν(C=C)	30.9	38.8	1.8	1.3
1553	ν(N-H/C=C)	49.4	35.8	2.5	1.5
1602	ν(C=C)	70.5	66.6	13.4	7.3
1642	ν(C=C)	67.5	63.3	5.5	4.7
1671	ν(C=C)	68.6	68.6	5.0	4.1
1721	ν(C=O)	—	18.3	—	0.4
1737	ν(C=O)	46.3	34.5	5.2	2.7

Abbreviation: ν, stretching vibrations.

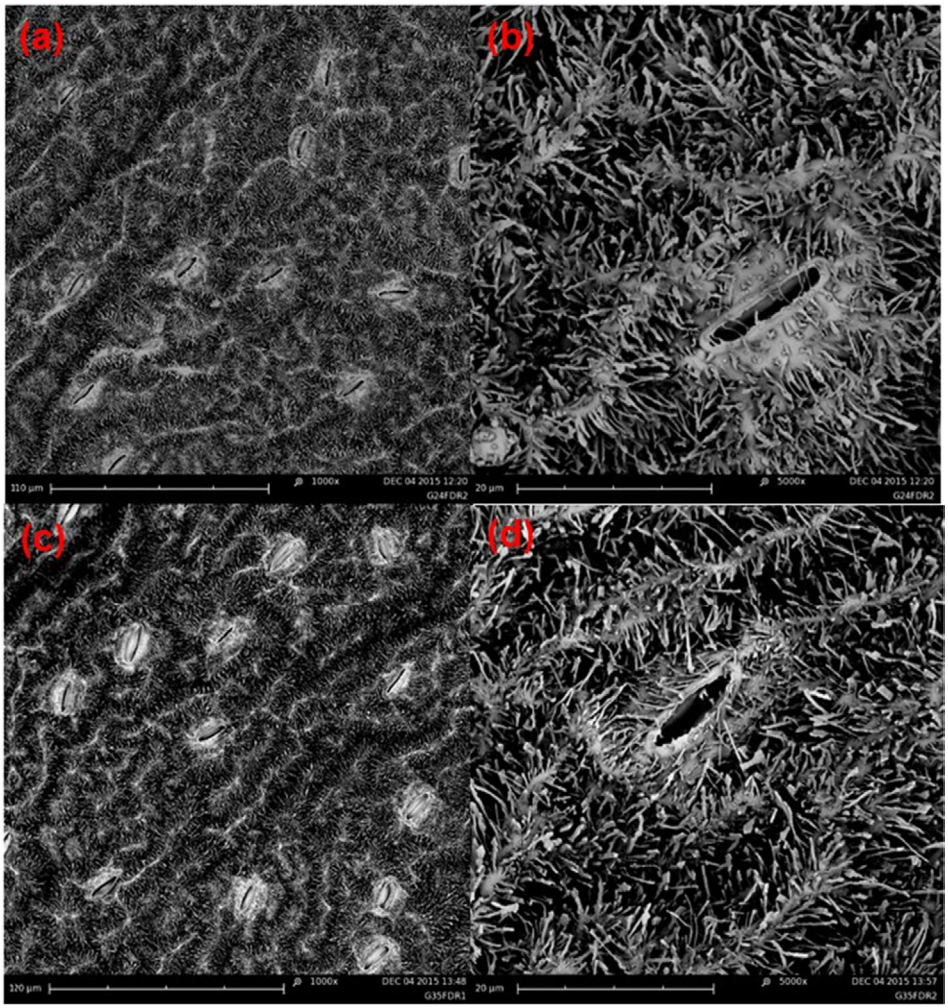


FIGURE 5 | Scanning electron microscope (SEM) images of leaf surface of *Pisum sativum* cv. CDC Golden from the 24/18°C day/night temperature (control) growth chamber (a, 1000× magnification; b, 5000× magnification) and from the 35/18°C day/night temperature (heat-treated magnification) growth chamber (c, 1000× magnification; d, 5000× magnification).

cutan, waxes, polysaccharides and phenolic components play crucial roles in response to heat stress.

Author Contributions

Yunfei Jiang: conceptualisation, data curation, formal analysis, investigation, methodology, visualisation, project administration, writing – original draft. Rachid Lahlali: conceptualisation, data curation, formal analysis, investigation, methodology, software, visualisation, writing – review and editing. **Rosalind Bueckert:** funding acquisition, investigation, resources, supervision, writing – review and editing. **Saroj Kumar:** formal analysis, software, visualisation, writing – review and editing. **Chithra Karunakaran:** resources, supervision, writing – review and editing.

Acknowledgements

This work was supported by Canadian Light Source Inc., Saskatchewan Agriculture Development Fund, Saskatchewan Pulse Growers Association, Western Grains Research Fund, the Natural Sciences and Engineering Research Council (NSERC) of Canada—CRD Program, the Canada Foundation for Innovation, the National Research Council Canada, the Canadian Institutes of Health Research, Western Economic Diversification Canada and the University of Saskatchewan. We acknowledge the kind help from the mid infrared beamline staff, Dr. Xia Liu, during experimental setup at Canadian Light Source. The authors thank Dustin MacLean for his assistance in language editing.

Conflicts of Interest

The authors declare no conflicts of interest.

Data Availability Statement

The data that support the findings of this study are available from the corresponding author upon reasonable request.

References

Asada, K. 2006. "Production and Scavenging of Reactive Oxygen Species in Chloroplasts and Their Functions." *Plant Physiology* 141, no. 2: 391–396.

Borchman, D., and S. Sinha. 2002. "Determination of Products of Lipid Oxidation by Infrared Spectroscopy." *Methods in Molecular Biology* 186: 21–28.

Bueckert, R. A., S. Wagenhoffer, G. Hnatowich, and T. D. Warkentin. 2015. "Effect of Heat and Precipitation on Pea Yield and Reproductive

Performance in the Field." *Canadian Journal of Plant Science* 95, no. 4: 629–639.

Carr, G. L. 2001. "Resolution Limits for Infrared Microspectroscopy Explored With Synchrotron Radiation." *Review of Scientific Instruments* 72, no. 3: 1613–1619.

Chai, X., S. Takayuki, X. Cao, Q. Guo, and Y. Zhao. 2007. "Spectroscopic Studies of the Progress of Humification Processes in Humic Substances Extracted From Refuse in a Landfill." *Chemosphere* 69, no. 9: 1446–1453.

Chen, L., N. C. Carpita, W. Reiter, R. H. Wilson, C. Jeffries, and M. C. McCann. 1998. "A Rapid Method to Screen for Cell-Wall Mutants Using Discriminant Analysis of Fourier Transform Infrared Spectra." *Plant Journal* 16, no. 3: 385–392.

Dokken, K. M., L. C. Davis, L. E. Erickson, S. Castro-Diaz, and N. S. Marinkovic. 2005. "Synchrotron Fourier Transform Infrared Microspectroscopy: A New Tool to Monitor the Fate of Organic Contaminants in Plants." *Microchemical Journal* 81, no. 1: 86–91.

Domínguez, E., J. A. Heredia-Guerrero, and A. Heredia. 2011. "The Biophysical Design of Plant Cuticles: An Overview." *New Phytologist* 189, no. 4: 938–949.

Dubis, E. N., A. T. Dubis, and J. Popławski. 2001. "Determination of the Aromatic Compounds in Plant Cuticular Waxes Using FT-IR Spectroscopy." *Journal of Molecular Structure* 596, no. 1–3: 83–88.

España, L., J. A. Heredia-Guerrero, P. Segado, J. J. Benítez, A. Heredia, and E. Domínguez. 2014. "Biomechanical Properties of the Tomato (*Solanum lycopersicum*) Fruit Cuticle During Development Are Modulated by Changes in the Relative Amounts of Its Components." *New Phytologist* 202, no. 3: 790–802.

FAOSTAT. 2024. "Crops and Livestock Products." Https://Www.Fao.Org/Faostat/En/#data/QCL.

Freitas, P. A. d. M., K. Iha, M. Felinto, and M. E. V. Suárez-Iha. 2008. "Adsorption of di-2-Pyridyl Ketone Salicyloylhydrazone on Amberlite XAD-2 and XAD-7 Resins: Characteristics and Isotherms." *Journal of Colloid and Interface Science* 323, no. 1: 1–5.

Gonzalez, R., N. D. Paul, K. Percy, et al. 1996. "Responses to Ultraviolet-B Radiation (280–315 Nm) of Pea (*Pisum sativum*) Lines Differing in Leaf Surface Wax." *Physiologia Plantarum* 98, no. 4: 852–860.

Goormaghtigh, E., J. M. Ruysschaert, and V. Raussens. 2006. "Evaluation of the Information Content in Infrared Spectra for Protein Secondary Structure Determination." *Biophysical Journal* 90, no. 8: 2946–2957. https://doi.org/10.1529/biophysj.105.072017.

Götz, A., R. Nikzad-Langerodi, Y. Staedler, A. Bellaire, and J. Saukel. 2020. "Apparent Penetration Depth in Attenuated Total Reflection Fourier-Transform Infrared (ATR-FTIR) Spectroscopy of *Allium cepa* L. Epidermis and Cuticle." *Spectrochimica Acta—Part A: Molecular and Biomolecular Spectroscopy* 224: 117460. https://doi.org/10.1016/j.saa.2019.117460.

Guzmán, P., V. Fernández, M. L. García, M. Khayet, A. Fernández, and L. Gil. 2014. "Localization of Polysaccharides in Isolated and Intact Cuticles of Eucalypt, Poplar and Pear Leaves by Enzyme-Gold Labelling." *Plant Physiology and Biochemistry* 76: 1–6.

Guzmán, P., V. Fernández, J. Graça, et al. 2014. "Chemical and Structural Analysis of Eucalyptus Globulus and *E. camaldulensis* Leaf Cuticles: A Lipidized Cell Wall Region." *Frontiers in Plant Science* 5: 481.

Hall, D. M., A. I. Matus, J. Lamberton, and H. N. Barber. 1965. "Infra-Specific Variation in Wax on Leaf Surfaces." *Australian Journal of Biological Sciences* 18, no. 2: 323–332.

Hardin, J. A. 2012. *In Situ Sensing of Leaf Cuticular Wax, Pecan Yield and Pecan Leaf Nitrogen Concentration*. Oklahoma State University.

Heraud, P., S. Caine, G. Sanson, R. Gleadow, B. R. Wood, and D. McNaughton. 2007. "Focal Plane Array Infrared Imaging: A New Way to Analyse Leaf Tissue." *New Phytologist* 173, no. 1: 216–225.

Heredia-Guerrero, J. A., J. J. Benítez, E. Domínguez, et al. 2014. "Infrared and Raman Spectroscopic Features of Plant Cuticles: A Review." *Frontiers in Plant Science* 5: 305.

Heredia-Guerrero, J. A., R. De Lara, E. Domínguez, A. Heredia, J. Benavente, and J. J. Benítez. 2012. "Chemical–Physical Characterization of Isolated Plant Cuticles Subjected to Low-Dose γ-Irradiation." *Chemistry and Physics of Lipids* 165, no. 8: 803–808.

Innes, S. N., L. E. Arve, B. Zimmermann, et al. 2019. "Elevated Air Humidity Increases UV Mediated Leaf and DNA Damage in Pea (*Pisum sativum*) due to Reduced Flavonoid Content and Antioxidant Power." *Photochemical and Photobiological Sciences* 18, no. 2: 387–399. https://doi.org/10.1039/C8PP00401C.

Isensee, K., N. Kröger-Lui, and W. Petrich. 2018. "Biomedical Applications of Mid-Infrared Quantum Cascade Lasers—A Review." *Analyst* 143, no. 24: 5888–5911. https://doi.org/10.1039/c8an01306c.

Jiang, Y., R. A. Bueckert, T. D. Warkentin, and A. R. Davis. 2017. "High Temperature Effects on In Vitro Pollen Germination and Seed Set in Field Pea." *Canadian Journal of Plant Science* 98, no. 1: 71–80. https://doi.org/10.1139/cjps-2017-0073.

Jiang, Y., A. R. Davis, V. Vujanovic, and R. A. Bueckert. 2019. "Reproductive Development Response to High Daytime Temperature in Field Pea." *Journal of Agronomy and Crop Science* 205, no. 3: 324–333. https://doi.org/10.1111/jac.12328.

Jiang, Y., A. R. Davis, T. D. Warkentin, and R. A. Bueckert. 2020. "Pea Pollen Viability and Seed Set Response at High Night Temperatures." *Canadian Journal of Plant Science* 100, no. 3: 332–335. https://doi.org/10.1139/cjps-2019-0060.

Jiang, Y., M. Diapari, R. A. Bueckert, B. Tar'an, and T. D. Warkentin. 2017. "Population Structure and Association Mapping of Traits Related to Reproductive Development in Field Pea." *Euphytica* 213, no. 9: 1–20. https://doi.org/10.1007/s10681-017-2006-1.

Jiang, Y., R. Lahlali, C. Karunakaran, S. Kumar, A. R. Davis, and R. A. Bueckert. 2015. "Seed Set, Pollen Morphology and Pollen Surface Composition Response to Heat Stress in Field Pea." *Plant, Cell & Environment* 38, no. 11: 2387–2397. https://doi.org/10.1111/pce.12589.

Jiang, Y., R. Lahlali, C. Karunakaran, T. D. Warkentin, A. R. Davis, and R. A. Bueckert. 2019. "Pollen, Ovules, and Pollination in Pea: Success, Failure, and Resilience in Heat." *Plant, Cell and Environment* 42, no. 1: 354–372. https://doi.org/10.1111/pce.13427.

Jiang, Y., D. L. Lindsay, A. R. Davis, et al. 2020. "Impact of Heat Stress on Pod-Based Yield Components in Field Pea (*Pisum sativum* L.)." *Journal of Agronomy and Crop Science* 206, no. 1: 76–89. https://doi.org/10.1111/jac.12365.

Johnson, E. J., O. Dorot, J. Liu, B. Chefetz, and B. Xing. 2007. "Spectroscopic Characterization of Aliphatic Moieties in Four Plant Cuticles." *Communications in Soil Science and Plant Analysis* 38, no. 17–18: 2461–2478.

Karuppanapandian, T., J.-C. Moon, C. Kim, K. Manoharan, and W. Kim. 2011. "Reactive Oxygen Species in Plants: Their Generation, Signal Transduction, and Scavenging Mechanisms." *Australian Journal of Crop Science* 5, no. 6: 709–725.

Khoddami, A., M. A. Wilkes, and T. H. Roberts. 2013. "Techniques for Analysis of Plant Phenolic Compounds." *Molecules* 18, no. 2: 2328–2375.

Król, A., R. Amarowicz, and S. Weidner. 2014. "Changes in the Composition of Phenolic Compounds and Antioxidant Properties of Grapevine Roots and Leaves (*Vitis vinifera* L.) Under Continuous of Long-Term Drought Stress." *Acta Physiologiae Plantarum* 36: 1491–1499.

Kumar, S. 2014. "Infrared Difference Spectroscopy as a Physical Tool to Study Biomolecules." *Applied Spectroscopy Reviews* 49, no. 3: 187–200.

Kumar, S., and A. Barth. 2010. "Phosphoenolpyruvate and Mg2+ Binding to Pyruvate Kinase Monitored by Infrared Spectroscopy." *Biophysical Journal* 98, no. 9: 1931–1940.

Lahlali, R., Y. Jiang, S. Kumar, et al. 2014. "ATR-FTIR Spectroscopy Reveals Involvement of Lipids and Proteins of Intact Pea Pollen Grains to Heat Stress Tolerance." *Frontiers in Plant Science* 5: 747. https://doi.org/10.3389/fpls.2014.00747.

Liu, N., C. Karunakaran, R. Lahlali, T. Warkentin, and R. A. Bueckert. 2019. "Genotypic and Heat Stress Effects on Leaf Cuticles of Field Pea Using ATR-FTIR Spectroscopy." *Planta* 249, no. 2: 601–613. https://doi.org/10.1007/s00425-018-3025-4.

Liu, N., L. Zhao, L. Tang, et al. 2020. "Mid-Infrared Spectroscopy Is a Fast Screening Method for Selecting Arabidopsis Genotypes With Altered Leaf Cuticular Wax." *Plant, Cell and Environment* 43, no. 3: 662–674. https://doi.org/10.1111/pce.13691.

Mantsch, H. H., P. W. Yang, A. Martin, and D. G. Cameron. 1988. "Infrared Spectroscopic Studies of *Acholeplasma laidlawii* B Membranes: Comparison of the Gel to Liquid-Crystal Phase Transition in Intact Cells and Isolated Membranes." *European Journal of Biochemistry* 178, no. 2: 335–341.

Martin, J. A., A. Solla, S. Woodward, and L. Gil. 2005. "Fourier Transform-Infrared Spectroscopy as a New Method for Evaluating Host Resistance in the Dutch Elm Disease Complex." *Tree Physiology* 25, no. 10: 1331–1338.

McCann, M. C., L. Chen, K. Roberts, et al. 1997. "Infrared Microspectroscopy: Sampling Heterogeneity in Plant Cell Wall Composition and Architecture." *Physiologia Plantarum* 100, no. 3: 729–738.

Møller, I. M., P. E. Jensen, and A. Hansson. 2007. "Oxidative Modifications to Cellular Components in Plants." *Annual Review of Plant Biology* 58, no. 1: 459–481.

Pellerin, C., C. M. Snively, D. B. Chase, and J. F. Rabolt. 2004. "Performance and Application of a New Planar Array Infrared Spectrograph Operating in the Mid-Infrared (2000–975 cm^{-1}) Fingerprint Region." *Applied Spectroscopy* 58, no. 6: 639–646.

Ribeiro da Luz, B. 2006. "Attenuated Total Reflectance Spectroscopy of Plant Leaves: A Tool for Ecological and Botanical Studies." *New Phytologist* 172, no. 2: 305–318.

Sadras, V. O., L. Lake, K. Chenu, L. S. McMurray, and A. Leonforte. 2012. "Water and Thermal Regimes for Field Pea in Australia and Their Implications for Breeding." *Crop and Pasture Science* 63, no. 1: 33–44. https://doi.org/10.1071/CP11321.

Shepherd, T., and D. Wynne Griffiths. 2006. "The Effects of Stress on Plant Cuticular Waxes." *New Phytologist* 171, no. 3: 469–499.

Sowa, S., K. F. Connor, and L. E. Towill. 1991. "Temperature Changes in Lipid and Protein Structure Measured by Fourier Transform Infrared Spectrophotometry in Intact Pollen Grains." *Plant Science* 78, no. 1: 1–9.

Szymanska-Chargot, M., and A. Zdunek. 2013. "Use of FT-IR Spectra and PCA to the Bulk Characterization of Cell Wall Residues of Fruits and Vegetables Along a Fraction Process." *Food Biophysics* 8: 29–42.

Tanino, K., I. R. Willick, K. Hamilton, et al. 2017. "Chemotyping Using Synchrotron Mid-Infrared and X-Ray Spectroscopy to Improve Agricultural Production." *Canadian Journal of Plant Science* 97, no. 6: 982–996.

Tanino, K. K., S. Kobayashi, C. Hyett, et al. 2013. "*Allium fistulosum* as a Novel System to Investigate Mechanisms of Freezing Resistance." *Physiologia Plantarum* 147, no. 1: 101–111.

Teng, X., M. Li, H. He, et al. 2024. "Mid-Infrared Photothermal Imaging: Instrument and Life Science Applications." *Analytical Chemistry* 96, no. 20: 7895–7906. https://doi.org/10.1021/acs.analchem.4c02017.

Van de Voort, F. R., A. A. Ismail, J. Sedman, and G. Emo. 1994. "Monitoring the Oxidation of Edible Oils by Fourier Transform Infrared Spectroscopy." *Journal of the American Oil Chemists' Society* 71: 243–253.

Villena, J. F., E. Domínguez, and A. Heredia. 2000. "Monitoring Biopolymers Present in Plant Cuticles by FT-IR Spectroscopy." *Journal of Plant Physiology* 156, no. 3: 419–422.

Wang, H., Q. Xie, and X. G. Xu. 2022. "Super-Resolution Mid-Infrared Spectro-Microscopy of Biological Applications Through Tapping Mode and Peak Force Tapping Mode Atomic Force Microscope." *Advanced Drug Delivery Reviews* 180: 114080. https://doi.org/10.1016/j.addr.2021.114080.

Wang, S., S. Dou, Z. Yu, L. Ma, Y. Li, and S. Yu. 2014. "Compositions and Properties of Microbial Residues Formed by Three Single Species Fungi and Mixed Strains in Cellulose-Containing Liquid Media." *Journal of Soil Science and Plant Nutrition* 14, no. 2: 366–381.

Willick, I. R., R. Lahlali, P. Vijayan, D. Muir, C. Karunakaran, and K. K. Tanino. 2018. "Wheat Flag Leaf Epicuticular Wax Morphology and Composition in Response to Moderate Drought Stress Are Revealed by SEM, FTIR-ATR and Synchrotron X-Ray Spectroscopy." *Physiologia Plantarum* 162, no. 3: 316–332.

Wróbel, M., M. Karama, R. Amarowicz, E. Fr czek, and S. Weidner. 2005. "Metabolism of Phenolic Compounds in *Vitis riparia* Seeds During Stratification and During Germination Under Optimal and Low Temperature Stress Conditions." *Acta Physiologiae Plantarum* 27: 313–320.

Yee, N., L. G. Benning, V. R. Phoenix, and F. G. Ferris. 2004. "Characterization of Metal– Cyanobacteria Sorption Reactions: A Combined Macroscopic and Infrared Spectroscopic Investigation." *Environmental Science & Technology* 38, no. 3: 775–782.